Acta Crystallographica Section D
Biological Crystallography
ISSN 0907-4449

Structure determination and analysis of acyl-CoA oxidase (ACX1) from tomato

Rachel A. Powers,[a] Christopher L. Rife,[a] Anthony L. Schilmiller,[a,b] Gregg A. Howe[a,b] and R. Michael Garavito[a]*

[a]Department of Biochemistry and Molecular Biology, Michigan State University, East Lansing, MI 48824, USA, and [b]Department of Energy–Plant Research Laboratory, Michigan State University, East Lansing, MI 48824, USA

Correspondence e-mail: garavito@msu.edu

Received 30 January 2006
Accepted 18 April 2006

PDB Reference: LeACX1, 2fon, r2fonsf.

The flavoenzyme acyl-CoA oxidase (ACX) catalyzes the first committed step in β-oxidation and is required for the biosynthesis of jasmonic acid, a signaling molecule involved in plant defense. Recently, a mutant in tomato was identified that is deficient in jasmonic acid production and compromised in its wound response. This results from a single point mutation in *acx1*, which causes the conserved residue Thr138 to be substituted by isoleucine. To understand the structural basis for this mutation, the crystal structure of LeACX1 was determined to 2.74 Å resolution by molecular replacement. Unexpectedly, an unusual packing arrangement was observed in which three monomers of LeACX1 are present in the asymmetric unit. Although the tertiary structure of LeACX1 is essentially similar to the previously determined structures of ACX enzymes, the packing within the unit cells is distinctly different.

1. Introduction

Oxylipins are lipid-derived bioactive signaling molecules synthesized *de novo* in response to environmental and developmental factors. The jasmonate family is particularly well characterized owing to their involvement in plant defense (Liechti & Farmer, 2002). In particular, jasmonic acid is crucial for proper wound response to mechanical injury. The complete biosynthesis of jasmonic acid is a complex multi-step process requiring a number of enzymes and the translocation of intermediates from the chloroplast to the peroxisome (Vick & Zimmerman, 1984; Schaller, 2001). The first committed as well as the rate-limiting step in the β-oxidation stage of this process is catalyzed by the flavoenzyme acyl-CoA oxidase (ACX). Several ACX isozymes exist; however, the ACX1 isozyme is believed to be responsible for wound-induced jasmonic acid synthesis (Cruz Castillo *et al.*, 2004; Li *et al.*, 2005). ACX1 catalyzes the peroxisomal β-oxidation of fatty-acid substrates, converting acyl-CoA to 2-*trans*-enoyl-CoA. For the production of jasmonic acid, three cycles of β-oxidation are required to shorten the length of the acyl chain of the precursor 12-oxo-phytodienoic acid by six C atoms. The mechanism occurs through two half-reactions, both of which are catalyzed by ACX1. In the first half-reaction, the cofactor flavin-adenine dinucleotide (FAD) is reduced to its $FADH^-$ form and a double bond is introduced between C^α and C^β of the fatty-acyl substrate. FAD is re-oxidized in the second half reaction by molecular oxygen and in the process the potential signaling molecule H_2O_2 is generated.

A recently discovered mutant in tomato (*Lycopersicon esculentum*) was described as being deficient in jasmonic acid production and compromised in its wound response to tobacco hornworm attack (Li *et al.*, 2005). A single point mutation in the *acx1* gene was determined to be the cause of this phenotype and emphasizes the essential role of ACX1 in wound signaling. The mutation results in Thr138 being replaced by an isoleucine. Thr138 is a conserved residue and previous structural work on ACX1 from both rat liver (Nakajima *et al.*, 2002) and *Arabidopsis thaliana* (Pedersen & Henriksen, 2005) observed that Thr138 $O^{\gamma 1}$ hydrogen bonds with the required cofactor FAD. In an effort to understand the structural basis for the Thr138Ile mutation, the crystal structure of LeACX1 from tomato was determined to 2.74 Å resolution by molecular replacement.

Table 1
Crystallographic summary for the structure of LeACX1.

Values in parentheses are for the highest resolution shell.

Unit-cell parameters (Å, °)	a = 120.20, b = 240.33, c = 89.30, $\alpha = \beta = \gamma = 90$
Resolution (Å)	2.70 (2.77–2.70)
Unique reflections	64138
Total observations	384325
R_{merge} (%)	9.2 (37.4)
Completeness† (%)	95.4 (99.8)
$\langle I\rangle/\langle\sigma(I)\rangle$	12.2 (5.1)
Resolution range for refinement (Å)	30–2.74
No. of protein residues	1963
No. of water molecules	36
R.m.s.d. bond lengths (Å)	0.018
R.m.s.d. bond angles (°)	1.9
R factor (%)	21.2
R_{free}‡ (%)	26.7
Average B factors	
Protein atoms	
Molecule A	67.9
Molecule B	68.1
Molecule C	71.5
FAD atoms	
Molecule A	55.3
Molecule B	50.2
Molecule C	99.8
Water molecules	57.6

† Fraction of theoretically possible reflections observed. ‡ R_{free} was calculated with 5% of reflections set aside randomly.

2. Experimental

2.1. Expression, purification and crystallization

LeACX1 was expressed and purified to homogeneity as described previously (Li *et al.*, 2005). Purified LeACX1 was concentrated to approximately 9 mg ml^{-1}. Crystals of LeACX1 were grown by vapor diffusion using the hanging-drop method in 100 m*M* Tris pH 8.0 with 10% 2-methyl-2,4-pentanediol, 7% polyethylene glycol 6000 and 1 m*M* acetyl-CoA. Prior to data collection, crystals were harvested with a nylon cryo-loop (Hampton Research, Aliso Viejo, CA, USA) and immediately flash-cooled in liquid nitrogen.

2.2. Data collection, structure determination and refinement

Data were measured on the COM-CAT beamline (32ID) of the Advanced Photon Source at Argonne National Laboratory at 100 K using a MAR CCD detector. Owing to significant radiation damage, reflections collected from two isomorphous crystals were processed, scaled and merged using the *HKL* package (Otwinowski & Minor, 1997) (Table 1).

The structure was determined by molecular replacement with *CNS* (Brünger *et al.*, 1998) using a single monomer of rat liver ACOII, which is approximately 42% identical to LeACX1, as the initial phasing model (PDB code 1is2; Nakajima *et al.*, 2002). All ligand atoms and water molecules were removed from the phasing model and residues from ACOII not matching LeACX1 were changed to alanines. The Matthews coefficient V_M was 2.18 Å^3 Da^{-1} for four monomers in the asymmetric unit, 2.90 Å^3 Da^{-1} for three monomers and 4.36 Å^3 Da^{-1} for two monomers. Since the biologically relevant molecule is a dimer and previously determined ACX structures crystallized with a dimer in the asymmetric unit, the molecular-replacement program was used to search for either two or four monomers. Using *CNS*, only two monomers could be placed. The initial dimer model was refined with *CNS* using the maximum-likelihood target and including a bulk-solvent correction and a 2.0σ cutoff. Cycles of manual rebuilding in *O* (Jones *et al.*, 1991) were performed with σ_A-weighted electron-density maps calculated in *CNS*. Inspection of the maps revealed additional electron density that seemed to correspond to protein not accounted for by the model. The molecular-replacement program *Phaser* (Read, 2001) successfully located a third monomer of ACX1 by fixing the initial dimer solution. The model containing three monomers was further refined using TLS parameters (Winn *et al.*, 2001) in *REFMAC*5 (Murshudov *et al.*, 1997; Collaborative Computational Project, Number 4, 1994).

3. Results and discussion

3.1. Unexpected packing arrangement of LeACX1

The biologically relevant entity of ACX1 is a dimer and the formation of this dimer is necessary for binding of the FAD cofactor since each monomer contributes to the formation of its binding site (Nakajima *et al.*, 2002). Related ACXs from rat liver (42% sequence identity) and *A. thaliana* (78% sequence identity) crystallized with the biological dimer in the asymmetric unit. Unexpectedly, LeACX1 crystallizes with three monomers (named *A*, *B* and *C*) in the asymmetric unit, essentially one full plus one half of a biological dimer (Fig. 1). Monomers *A* and *B* form a biological dimer related by non-crystallographic symmetry, whereas monomer *C* forms a biological dimer with its symmetry mate across a crystallographic twofold axis (Fig. 1). FAD is observed to bind to each of the monomers (Fig. 2). The *C* monomer appears to be less well ordered overall than the *A* and *B* monomers as evidenced by poorer electron density and higher *B* factors throughout the entire monomer, including the FAD (Table 1; Fig. 2). Although this crystal-packing arrangement is not common, it has been observed previously (Holden & Banaszak, 1983; Kerfeld *et al.*, 1998). However, in this case two local twofolds are

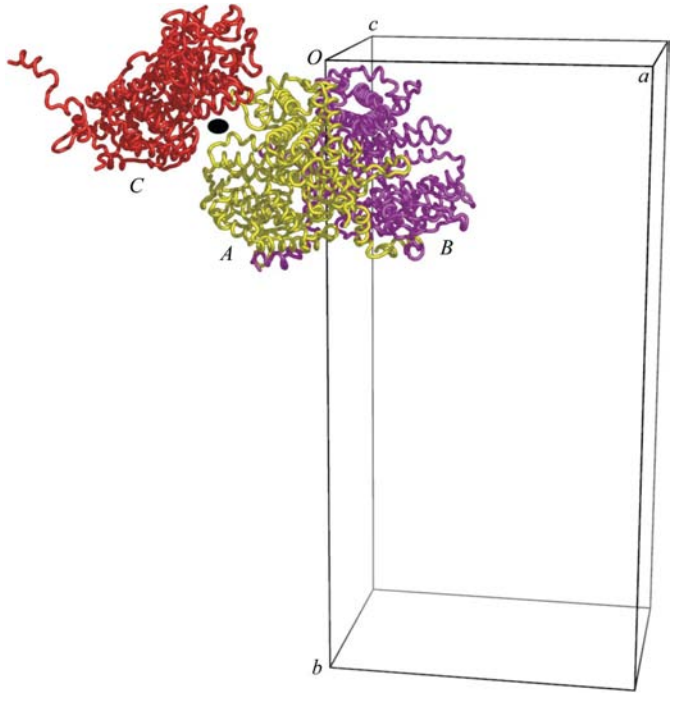

Figure 1
Representation of the unusual packing arrangement of LeACX1 with three monomers, essentially one full and one half of the biological dimer, in the asymmetric unit. The third monomer in the asymmetric unit (*C*) forms a dimer across a crystallographic twofold (denoted by a black oval), thereby generating the homodimeric biological molecule. All figures were created with *PyMOL* (DeLano, 2002).

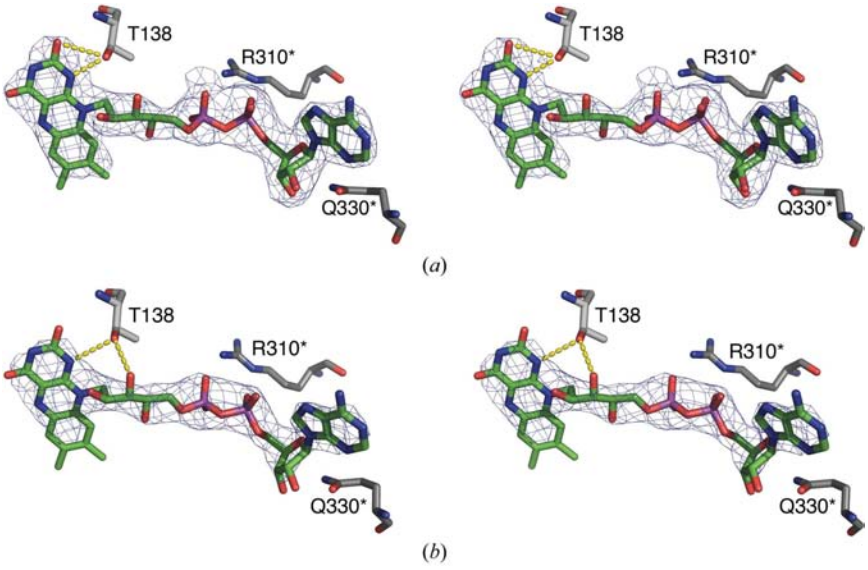

Figure 2
Refined $2F_o - F_c$ electron-density map for the cofactor FAD contoured at 1.0σ. (*a*) Monomer *A*, which also resembles that of monomer *B*. (*b*) Monomer *C*. The poor electron density for FAD in the *C* monomer is representative of the disorder observed throughout the entire monomer. Dashed yellow lines indicate potential hydrogen bonds with Thr138. N atoms are colored blue, O atoms red and P atoms magenta. Carbon atoms of FAD are colored green. Protein C atoms are colored white for residues from the defining monomer (*A*, *B* and *C*) and gray for residues from its dimeric partner (*B*, *A* and *C**, respectively).

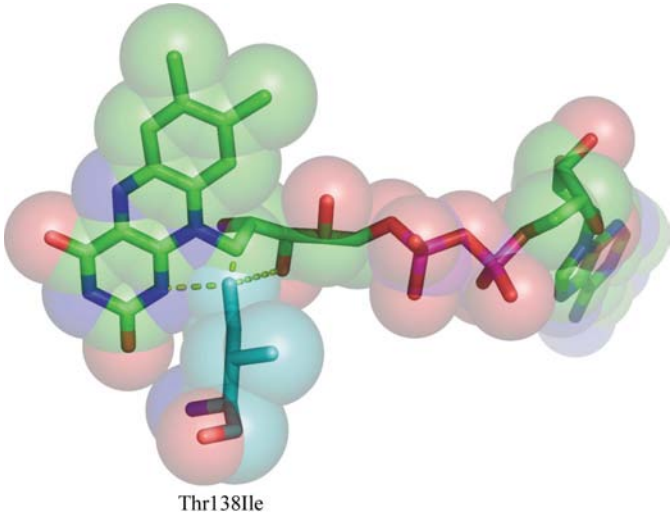

Figure 3
A model of the point mutant Thr138Ile suggests the structural basis for the compromised wound response exhibited by the mutant. Steric clashes are observed between the $C^{\delta1}$ atom of the modeled Ile (C atoms colored cyan) and atoms N1, C1* and O3* of FAD. Modeling of isoleucine was performed with *O*. The most favored conformation of this residue was chosen from the side-chain rotamer database (Kleywegt & Jones, 1998) supplied with the program.

observed in the self-rotation function. The stronger peak coincides with the molecular dyad between *A* and *B*, whereas a weaker peak is seen for the molecular dyad between *A* and *C* of LeACX1, which lies collinear with the crystallographic twofold axis.

To explain the unusual packing arrangement found in LeACX1, we analyzed the residues and interactions found at the unique interface of monomers *A* and *C*. Favorable interactions at the *AC* interface might drive the formation of the observed packing arrangement in the unit cell. Two sets of loops approach one another at this interface and were analyzed further. The residues in these loops, while not identical when compared with AtACX1, are essentially equivalent. Therefore, the different packing arrangement cannot be explained by favorable interactions at the *AC* interface of LeACX1. Considering the high sequence identity between the two enzymes, it is not surprising that no major differences exist on the surface that might explain the formation of a unique *AC* interface. Regardless of the lack of sequence differences, the closest distance across the interface at these loops is 3.9 Å and a more average separation is around 5 Å. This is likely to be too far to contribute much to driving the association of the *A* and *C* monomers.

Although produced under different conditions, AtACX1 crystallizes in space group $P2_12_12_1$, whereas LeACX1 crystallizes in space group $P2_12_12$. The unit-cell parameters are also somewhat related: for AtACX1, a = 85.6, b = 117.0, c = 131.3 Å (unit-cell volume of 1 314 995 Å^3), and for LeACX1, a = 120.2, b = 240.3, c = 89.3 Å (unit-cell volume of 2 579 346 Å^3). This doubling of the unit-cell size for LeACX1 arises mostly from a doubling in the length of b, but is only large enough to accommodate a third monomer, not another complete dimer.

The two molecular dimers observed in this crystal habit are essentially identical. From a biochemical viewpoint, formation of a dimer is absolutely required for FAD binding and hence enzyme activity. Additionally extensive and intimate associations occur at the dimer interface, burying 7100 Å^2 of accessible surface area in the LeACX1 dimer structure (calculated with *AREAIMOL* from *CCP*4). Thus, the packing of LeACX1 molecules in the crystal conforms to the constraints imposed by its unit-cell volume by including only three monomers in the asymmetric unit, while concomitantly satisfying the constraint for dimer formation by having the second biological dimer sit on a crystallographic twofold axis.

3.2. Analysis of the Thr138Ile mutant

The LeACX1 mutant T138I is compromised in wound-response signaling owing to a deficiency in jasmonic acid synthesis. Previous structural studies on related acyl-CoA oxidases observed that Thr138 $O^{\gamma1}$ made hydrogen bonds with cofactor FAD and was believed to play a role in correctly positioning FAD in the active site (Nakajima *et al.*, 2002; Pedersen & Henriksen, 2005). In the LeACX1 structure, hydrogen bonds between Thr138 $O^{\gamma1}$ and FAD are also observed (Fig. 2). Modeling the bulkier and hydrophobic isoleucine at this position indicates this mutation could occlude binding of FAD owing to the loss of hydrogen-bonding capability and steric collisions with FAD (Fig. 3). Spectroscopic experiments support this hypothesis, indicating that FAD is indeed not bound in the mutant protein (Li *et al.*, 2005).

4. Summary

ACX is an essential enzyme in the biosynthetic pathway of jasmonic acid, a signaling molecule involved with wound-induced plant defense. Here, we report the crystal structure of LeACX1 from tomato, which crystallizes in an unusual and unexpected fashion. Three monomers, a 'dimer and a half', are observed in the asymmetric

unit, but the overall packing in the unit cell generates identical molecular dimers, as expected, since dimer formation is required for cofactor binding and activity. Additionally, modeling of the jasmonic acid-deficient mutant identified in tomato (Thr138Ile) supports experimental data that FAD binding is occluded.

This work was supported by R01-GM65501 from the National Institutes of Health (to RMG). We thank K. Padmanabhan for helpful discussions regarding this manuscript. Use of the COM-CAT 32-ID beamline at the Advanced Photon Source was supported by the US Department of Energy, Office of Science, Office of Basic Energy Sciences under Contract No. W-31-109-Eng-38.

References

Brünger, A. T., Adams, P. D., Clore, G. M., DeLano, W. L., Gros, P., Grosse-Kunstleve, R. W., Jiang, J.-S., Kuszewski, J., Nilges, M., Pannu, N. S., Read, R. J., Rice, L. M., Simonson, T. & Warren, G. L. (1998). *Acta Cryst.* D**54**, 905–921.

Collaborative Computational Project, Number 4 (1994). *Acta Cryst.* D**50**, 760–763.

Cruz Castillo, M., Martinez, C., Buchala, A., Metraux, J. P. & Leon, J. (2004). *Plant Physiol.* **135**, 85–94.

DeLano, W. L. (2002). *The PyMOL Molecular Graphics System*, v.0.98. http://www.pymol.org.

Holden, H. M. & Banaszak, L. J. (1983). *J. Biol. Chem.* **258**, 2383–2389.

Jones, T. A., Zou, J. Y., Cowan, S. W. & Kjeldgaard, M. (1991). *Acta Cryst.* A**47**, 110–119.

Kerfeld, C. A., Salmeen, A. E. & Yeates, T. O. (1998). *Biochemistry*, **37**, 13911–13917.

Kleywegt, G. J. & Jones, T. A. (1998). *Acta Cryst.* D**54**, 1119–1131.

Li, C., Schilmiller, A. L., Liu, G., Lee, G. I., Jayanty, S., Sageman, C., Vrebalov, J., Giovannoni, J. J., Yagi, K., Kobayashi, Y. & Howe, G. A. (2005). *Plant Cell*, **17**, 971–986.

Liechti, R. & Farmer, E. E. (2002). *Science*, **296**, 1649–1650.

Murshudov, G. N., Vagin, A. A. & Dodson, E. J. (1997). *Acta Cryst.* D**53**, 240–255.

Nakajima, Y., Miyahara, I., Hirotsu, K., Nishina, Y., Shiga, K., Setoyama, C., Tamaoki, H. & Miura, R. (2002). *J. Biochem. (Tokyo)*, **131**, 365–374.

Otwinowski, Z. & Minor, W. (1997). *Methods Enzymol.* **276**, 307–326.

Pedersen, L. & Henriksen, A. (2005). *J. Mol. Biol.* **345**, 487–500.

Read, R. (2001). *Acta Cryst.* D**57**, 1373–1382.

Schaller, F. (2001). *J. Exp. Bot.* **52**, 11–23.

Vick, B. A. & Zimmerman, D. C. (1984). *Plant Physiol.* **75**, 458–461.

Winn, M. D., Isupov, M. N. & Murshudov, G. N. (2001). *Acta Cryst.* D**57**, 122–133.